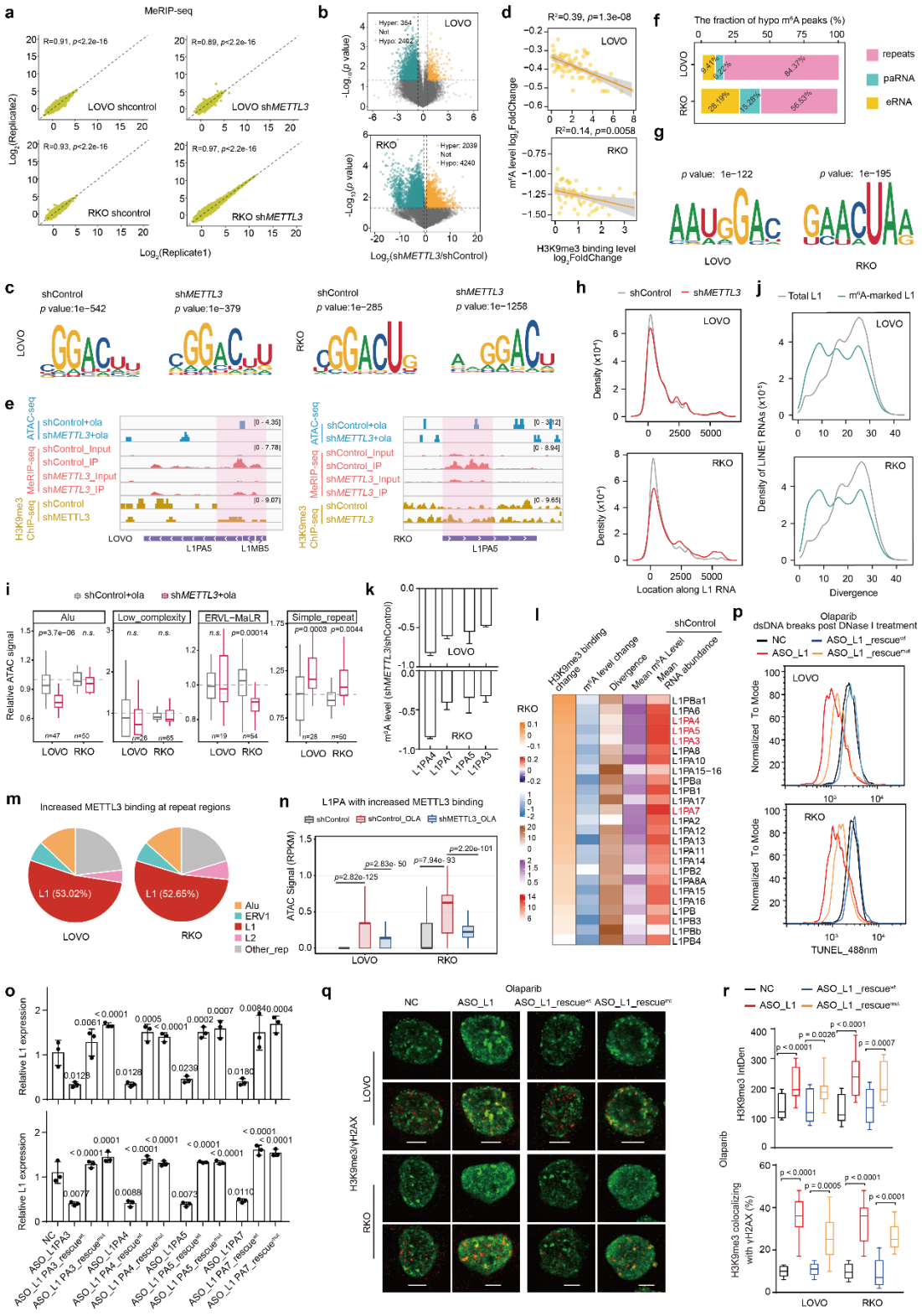

Fig. S4 METTL3-mediated m^{6}A modification of L1PA RNA regulates H3K9me3-dependent chromatin accessibility. (a) The correlation of m^{6}A levels on m^{6}A peak regions between two replicates showed high reproducibility. The R value refers to Pearson's correlation coefficient. **(b)** Scatter plots showing differential m^{6}A peaks in *METTL3*-knockdown LOVO and RKO cells compared with control cells using caRNA MeRIP-seq data. Each point represents a peak. Hypermethylated (m^{6}A $\log_2$

[fold change] > 0.58 and $P < 0.05$) and hypomethylated (m^6A log_2 [fold change] < -0.58 and $P < 0.05$) peaks are shown in yellow and green, respectively. **(c)** Enriched consensus motifs of m^6A peaks identified in *METTL3*-knockdown and control LOVO and RKO cells. *P* values were obtained by HOMER. **(d)** Correlation between changes in H3K9me3 binding and changes in m^6A levels on m^6A peaks following *METTL3* knockdown using caRNA MeRIP-seq and H3K9me3 ChIP-seq data. *R* refers to Pearson's correlation coefficient. **(e)** Integrative Genomics Viewer displaying decreased chromatin accessibility and m^6A levels as well as increased H3K9me3 binding following *METTL3* knockdown. **(f)** Bar plot showing the percentage of hypo-m^6A peaks (m^6A log_2 [sh*METTL3*/shControl] < -0.58 and $P < 0.05$) distributed at different chromosome-associated regulatory RNA species in LOVO and RKO cells. **(g)** Enriched consensus motifs of m^6A peak on LINE1 RNAs identified in control LOVO and RKO cells. *P* values were obtained by HOMER. **(h)** Metagene profiles of m^6A peaks along LINE1 RNAs on chromatin following *METTL3* knockdown. m^6A density decreased around the 5′end of LINE1 RNAs. **(i)** Boxplots showing releative ATAC signal on various repeat families with hypo-m^6A peaks (m^6A log_2 [sh*METTL3*/shControl] < -0.58 and $P < 0.05$) following *METTL3* knockdown in olaparib-treated LOVO and RKO cells. The releative ATAC signal was normalized by setting the average ATAC signal for each repeats in the shControl+olaparib group to 1. **(j)** Density plot showing the distribution of m^6A peaks on LINE1 RNAs with different evolutionary divergence. Error bars indicate mean ± SEM. **(k)** Relative m^6A levels of L1 quantified with RT-qPCR in *METTL3*-knockdown and control LOVO and RKO cells. **(l)** LINE1 RNAs belonging to the L1PA and L1PB subfamilies on chromatin. Heatmaps show changes in H3K9me3 binding levels and m^6A levels following *METTL3* knockdown, the divergence of LINE1 subfamilies, and the average m^6A levels and RNA abundance in control RKO cells, respectively. **(m)** The proportion of differentially increased METTL3 peaks (wild-type+olaparib versus wild-type+DMSO; log_2Fold change > 3) overlapped with different repeat families. **(n)** Boxplots summarizing changes in ATAC signals on L1PA elements that showed increased METTL3 binding upon olaparib treatment. **(o)** Knockdown efficiency of ASO targeting L1PA RNA was assessed by qPCR. **(p)** Genome-wide chromatin accessibility was analyzed by TUNEL-DNase I flow cytometry in control, L1PA RNA-knockdown, and L1PA RNA-knockdown cells rescued with wild-type (m^6A-wt) or m^6A-site mutant (m^6A-mut) L1PA RNA. **(q)** Immunofluorescence staining was performed to examine global and DNA damage site-specific histone modifications in control, L1PA RNA-knockdown, and rescued cells (with m^6A-wt or m^6A-mut L1PA RNA). Cells were co-stained with anti-γ-H2AX (red) and anti-H3K9me3 (green) antibodies. Scale bar: 5 μm. **(r)** Fluorescence signal intensity was quantified using ImageJ software. **(k, o, r)** Statistical analyses were performed using a *t* test. $n = 3$ biological replicates. Data are shown as mean ± SEM. **(a, b, d, i, n)** *P* values were calculated by Student's *t* test. *n.s.*: not significant. $n = 2$ biological replicates. Data are shown as mean ± SEM.